HYPERBOLIC SHEARLETS

Glenn R. Easley[1], *Demetrio Labate*[2], *Vishal M. Patel*[3]

[1]System Planning Corporation, Arlington, VA 22201
[2]Deptartment of Mathematics, University of Houston, Houston, TX 77204
[3]Center for Automation Research, University of Maryland, College Park, MD 20742
geasley@sysplan.com, dlabate@math.uh.edu, pvishalm@umiacs.umd.edu

ABSTRACT

Wavelets with composite dilations extend the traditional wavelet approach by allowing for the construction of waveforms defined not only at various scales and locations but also according to various orthogonal transformations. The shearlets, which yield optimally sparse representations for a large class of 2D and 3D data is the most widely known example of wavelets with composite dilations. However, many other useful constructions are obtained within this framework. In this paper, we examine the hyperbolic shearlets, a variant of the shearlet construction obtained as a system of well localized waveforms defined at various scales, locations and orientations, where the directionality is controlled by orthogonal transformations producing a sort of shearing along hyperbolic curves. The effectiveness of this new representation is illustrated by applications to image denoising. Our results compare favourably against similar denoising algorithms based on wavelets, curvelets and other sophisticated multiscale representations.

Index Terms— Wavelets with composite dilations, directional wavelets, multiresolution analysis, shearlets, contourlets.

1. INTRODUCTION

Among the different methods proposed during the last decade to overcome the limitations of traditional multiscale representations in dealing with multidimensional data [1], [2], wavelets with composite dilations offer a particularly general framework which allows one to derive a variety of powerful data representation schemes. *Wavelets with composite dilations*, originally introduced in [3, 4], are defined as the collections of functions in $L^2(\mathbb{R}^n)$ of the form

$$\{\psi_{j,\ell,k} = |\det A|^{j/2}\, \psi(B_\ell A^j \cdot -k) : j \in \mathbb{Z}, \ell \in \Lambda, k \in \mathbb{Z}^n\},$$

where $\psi \in L^2(\mathbb{R}^n)$, A is an expanding invertible $n \times n$ matrix, B_ℓ is a matrix for which $|\det B_\ell| = 1$ and Λ is a countable indexing set. In this approach, the matrices A^j are associated with scaling transformations and the matrices B_ℓ are associated with various orthogonal transformations. As a result, it is possible to construct a variety of systems which go far beyond traditional wavelets with respect to their ability to deal with the geometry of the data.

A particularly important example of wavelets with composite dilations are the *shearlets* which, in dimensions $n = 2$, are obtained by using anisotropic dilation matrices and shearlet matrices of the form

$$B_\ell = \begin{pmatrix} 1 & 1 \\ 0 & 1 \end{pmatrix}^\ell \text{ and } \tilde{B}_\ell = \begin{pmatrix} 1 & 0 \\ 1 & 1 \end{pmatrix}^\ell.$$

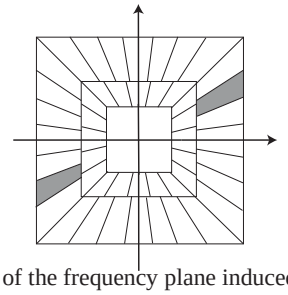

Fig. 1. The tiling of the frequency plane induced by the shearlets.

The shearlet tiling of the frequency plane is shown in Fig. 1. Thanks to their ability to deal with anisotropic features efficiently, shearlets provide nearly optimally sparse representations for a large class of images [5] and have been successfully applied to a variety of imaging applications [6, 7, 8, 9, 10].

Many other useful constructions besides shearlets can be obtained within the framework of wavelets with composite dilations. In fact, even the contourlets [11] and some of their variants can be derived from this approach, as recently observed in [12]. We refer to [12, 13] for additional constructions, including the illustration of their potential in image processing applications.

The goal of this paper is to examine the so-called *hyperbolic shearlets*, a special construction derived from the framework of wavelets with composite dilations which was originally introduced in [13] as a variant of the shearlets. Thanks to the special geometric properties of this construction which will be illustrated in this paper, it is anticipated that the applications of this new multiscale representation can have a high impact on deconvolution and other image enhancement tasks, as indicated by the novel decompositions suggested in [14] and by the techniques for dealing with motion blur recently proposed in [15].

The organization of the paper is as follows. After defining the hyperbolic shearlets in Section 2, their discrete implementation is presented in Section 3. We demonstrate experimental results in Section 4 and conclude with a brief discussion in Section 5.

2. HYPERBOLIC SHEARLETS

The system of hyperbolic shearlets is obtained from the wavelets with composite dilations (1), in dimension $n = 2$, by using the *hy-*

D.L. acknowledges support from NSF grants DMS 1005799 and DMS 1008900. V.M.P was partially supported by an ONR grant N00014-12-1-0124.

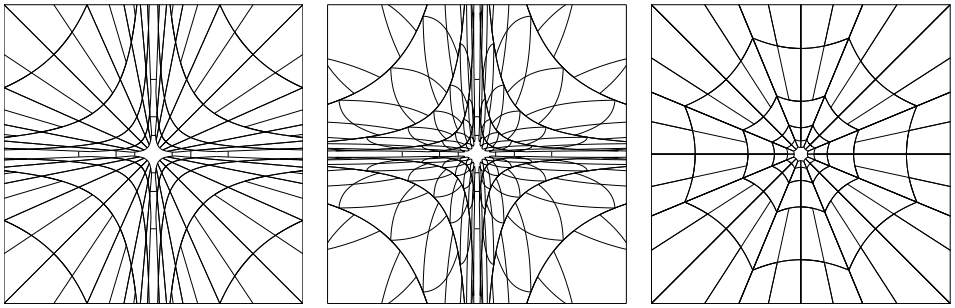

(a) (b) (c)

Fig. 2. Tiling of the frequency domain associated with an hyperbolic system of wavelets with composite dilations. (a) The starting shape S is a rectangle. (b) The starting shape S is a trapezoid. (c) The starting shape S is a rectangle and cone restricted set of filters are rotated around the origin.

perbolic matrices

$$B_\ell = \{b_\ell = \begin{pmatrix} \lambda^{-\ell} & 0 \\ 0 & \lambda^\ell \end{pmatrix} : \ell \in \mathbb{Z}\},$$

where $\lambda > 1$ is a fixed parameter; for the dilations matrices, it is possible to choose the isotropic dilation matrix $A = \begin{pmatrix} \sqrt{2} & 0 \\ 0 & \sqrt{2} \end{pmatrix}$ or the parabolic dilations matrix $A = \begin{pmatrix} 2 & 0 \\ 0 & \sqrt{2} \end{pmatrix}$ which is used in the shearlet construction. The construction resulting from these choices of matrices can be interpreted as a transformation of the shearlet tiling (see Fig. 1) under a nonlinear change of coordinates. In the following, we will set $\lambda = \sqrt{2}$, but the discussion below can be easily extended to other choices for λ.

For each $k > 0$, the set $H_k = \{(\xi_1, \xi_2) \in \widehat{\mathbb{R}}^2 : \xi_1\xi_2 = k\}$ consists of two branches of hyperbolas. Notice that, for any $\xi = (\xi_1, \xi_2) \in H_k$, every other point ξ' on the same branch of hyperbola has the unique representation $\xi' = (\xi_1\gamma^{-t}, \xi_2\gamma^t)$, where $\gamma > 1$ is fixed, for some $t \in \mathbb{R}$. This means any $\xi = (\xi_1, \xi_2)$ in the first quadrant can be parametrized by

$$\xi(r, t) = (\sqrt{r}\,(\sqrt{2})^{-t}, \sqrt{r}\,(\sqrt{2})^t),$$

where $r \geq 0$, $t \in \mathbb{R}$. This implies that

$$r = \xi_1\,\xi_2, \quad 2^t = \frac{\xi_2}{\xi_1}.$$

For any $k_1 < k_2$, a set $\{\xi(r, t) : k_1 \leq r < k_2\}$ is an *hyperbolic strip* and, for $m_1 < m_2$, a set $\{\xi(r, t) : k_1 \leq r < k_2, m_1 \leq 2^t \leq m_2\}$ is an *hyperbolic trapezoid*.

For any $k \neq 0$, the action of B_ℓ on the right preserves the hyperbolas H_k since

$$\begin{aligned} \xi\, B_\ell &= (\xi_1, \xi_2) \begin{pmatrix} (\sqrt{2})^{-\ell} & 0 \\ 0 & (\sqrt{2})^\ell \end{pmatrix} \\ &= (\xi_1(\sqrt{2})^{-\ell}, \xi_2(\sqrt{2})^\ell) \\ &= (\eta_1, \eta_2), \end{aligned}$$

and $\eta_1\eta_2 = \xi_1\xi_2$. Hence, the right action of the matrices B_ℓ maps an hyperbolic strip into itself.

Consider the action of the dilation matrices A^i, for $i \in \mathbb{Z}$, where A is one of the examples provided above. It is easy to verify that A maps the hyperbola $\xi_1\xi_2 = k$ to a new hyperbola. For example, if

$$A = \{a^i = \begin{pmatrix} \sqrt{2} & 0 \\ 0 & \sqrt{2} \end{pmatrix}^i : i \in \mathbb{Z}\},$$

A maps the hyperbola $\xi_1\xi_2 = k$ to the the hyperbola $\xi_1\xi_2 = 2k$, so that A^i maps the hyperbolic strip $\{\xi(r, t) : 1 \leq r < 2\}$ to the hyperbolic strip $\{\xi(r, t) : 2^i \leq r < 2^{i+1}\}$. By defining a set of generators Ψ consisting of appropriate characteristic sets in the frequency domain, it can be established that the hyperbolic system of wavelets with composite dilations

$$\{D_A^i D_{B_\ell}\, T_k\, \Psi : k \in \mathbb{Z}^2, \ell \in \mathbb{Z}\}$$

is a Parseval frame of $L^2(\mathbb{R}^2)$ which implies its transform is invertible and well-conditioned. We refer to [13] for additional detail about this construction.

Notice that, as the value ℓ increases in magnitude, the hyperbolic trapezoids become increasingly narrow and asymptotically approach either the horizontal or the vertical axis. Hence, to realize the system in the finite discrete setting, the indices i and ℓ can be limited to a finite range and the asymptotic regions not covered because of this discretization can then be dealt with by partitioning up the complement with a Laplacian Pyramid filtering. An example of the tiling of the frequency plane associated with this construction is illustrated in Fig. 2(a). Simple modifications of this construction lead to the frequency tilings shown in Fig. 2(b)-(c).

3. IMPLEMENTATION

The hyperbolic shearlets are implemented by designing a collection of filters $\{G_{j,\ell}\}$ that correspond to the appropriate elements of the hyperbolic shearlet system $\{\psi_{j,\ell,k} = |\det A|^{j/2}\,\psi(B_\ell A^j \cdot -k)\}$. These filters are derived by directly applying the matrices A^j and B_ℓ to a sequence of filter values to generate the specific spatial frequency tiling associated with the hyperbolic system $\mathcal{A}_{AB}(\Psi)$. Appropriate window adjustments are done by keeping track of the multiple assigned location points due to the pixelation. Examples of this construction are shown in Fig. 3 and an example of a hyperbolic filter in both time and frequency domain is shown in Fig. 4.

The synthesis filters are found by using the techniques given in [16, 17, 18, 19, 20, 21], which solve the multi-channel deconvolution problem (MDP). In 1983, Berenstein *et al.* considered the following MDP: *Given a collection $\{h_i\}_{i=0}^{m-1}$ of finite impulse response filters on $\mathbb{R}^d$ $(d \geq 2)$, find a collection $\{\tilde{h}_i\}_{i=0}^{m-1}$ of finite impulse response filters such that $\sum_{i=0}^{m-1} h_i * \tilde{h}_i = \delta$, where δ is a Dirac delta function.* This equation in the Fourier-Laplace domain is known as the analytic Bezout equation. The recent methods for solving the MDP in a discrete setting provide a more effective way of constructing appropriate synthesis filters [19],[20]. Thus, using these methods,

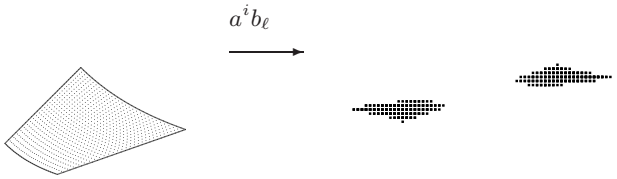

Fig. 3. Illustrations of filter constructions where the number of samples used are small for the purpose of presentation. The images on the left are the sequences of points $\{(\xi_1^n, \xi_2^n)\}_{n=1}^N$ contained in the region S. The images on the right are the sequences of points $\{(\overline{\eta}_1^n, \overline{\eta}_2^n)\}_{n=1}^N$ where $(\overline{\eta}_1^n, \overline{\eta}_2^n) = \lceil (\xi_1^n, \xi_2^n) a^i b_\ell \rceil$.

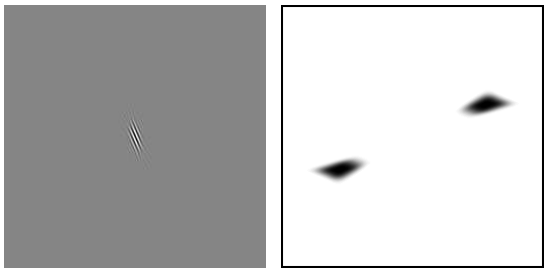

(a) (b)

Fig. 4. An example of a hyperbolic filter. (a) Time Domain. (b) Frequency Domain.

we are no longer constrained in the traditional ways to create higher dimensional directional analysis and synthesis filters. Additional detail about this implementation are found in [13] and [21].

4. EXPERIMENTAL RESULTS

In this section, we present numerical experiments on image restoration to demonstrate the effectiveness of the hyperbolic shearlet representation and its corresponding discrete implementations. We illustrate the denoising capability of these discrete transforms by means of hard thresholding. Recall that the *hard thresholding algorithm* consists in setting to zero the transform coefficients whose absolute values fall below a certain threshold T which depends on the standard deviation of the noise σ. Although hard thresholding is a rather crude form of thresholding and more sophisticated methods such as [7] are available, this method is a good indication of the potential of a transform in image restoration applications. Note that the point of this paper is not to extensively study the denoising capabilities of hyperbolic shearlets but rather to illustrate the flexibility of the framework of composite wavelets to generate useful and effective directional representations and its competitiveness against other transform-based methods. A more extensive comparison with other denoising algorithms including methods which are not transform-based will be addressed elsewhere.

Given noisy observations $y = x + n$, where n is zero-mean white Gaussian noise with variance σ^2, the objective is to estimate x. By adapting the standard wavelet shrinkage approach [22], we apply hard thresholding on the subband coefficients of the various decompositions. In particular, we choose the threshold $T_j = K\sigma_j$, where σ_j^2 is the noise variance in each subband and K is a constant. We set $K = 2$ for all subbands.

To assess the denoising performance of our method, we compare it against three different competing discrete multiscale transforms: the nonsubsampled wavelet transform, denoted by NSWT, the curvelet transform [23], denoted by curv, and the nonsubsampled contourlet transform [11], denoted by NSCT. We implemened each transform to 4 decomposition levels and we choose the thresholds to be $T_j = K\sigma_j$, where σ_j^2 is the noise variance in each subband and K is a constant. For these competing transforms, we choose $K = 4$ for the highest subband and $K = 3$ for the other subbands as done in [11].

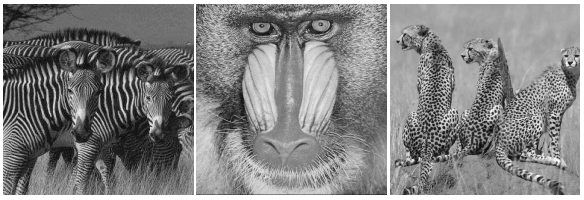

Fig. 5. Images used for the experiments. From left to right: *Zebra* (256×256), *Baboon* (512×512), and *Leopards* (512×512).

The discrete hyperbolic shearlet transforms we tested are the cone-based hyperbolic transform (c-hyper) shown in Fig. 2 (c) and the hyperbolic transform (hyper) shown in Fig. 2 (a). We used the peak signal-to-noise ratio (PSNR) to measure the performance of different transforms. Recall that, given an $N \times N$ image x and its estimate $\tilde{x}$, the PSNR in decibels (dB) is defined as

$$PSNR = 20 \log_{10} \frac{255N}{\|x - \tilde{x}\|_F},$$

where $\|.\|_F$ is the Frobenius norm.

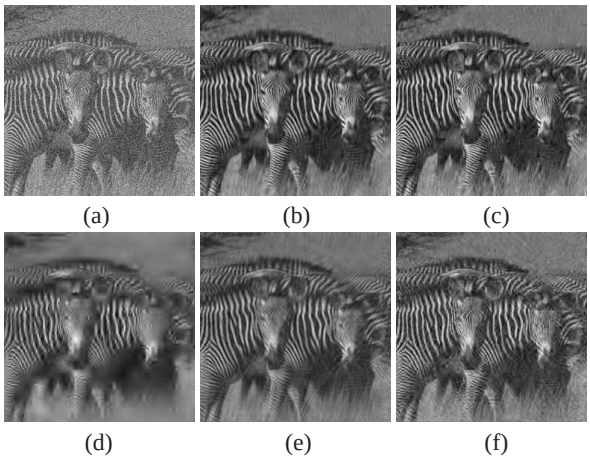

(a) (b) (c)

(d) (e) (f)

Fig. 6. Denoising results. (a) Noisy image with $\sigma = 30$, PSNR= 18.56 dB. (b) c-hyper estimate, PSNR= 24.67 dB. (c) hyper estimate, PSNR= 24.38 dB. (d) NSWT estimate, PSNR= 21.41 dB. (e) curv estimate, PSNR= 22.26 dB. (f) NSCT estimate, PSNR= 23.69 dB.

In Tables I, II and III, we show the results obtained by various decompositions on a *Zebra*, *Baboon* and a *Leopards* image, respectively. These images are shown in Fig. 5. The highest PSNR for each experiment is shown in bold. As it can be seen from the tables, all of the new transforms provide superior or comparable results to that obtained using NSWT, NSCT and curvelets. Indeed, in some cases, the hyperbolic shearlets provide improvement of nearly 1 dB or more compared to the competing transforms.

Fig. 6 shows the denoised *Zebra* image obtained with the various transforms. Note that the hyperbolic shearlets exhibits much better reconstructions of edge and curve features thus attesting the effectiveness of the proposed transform. Further results and comparisons on image denoising and image enhancement can be found in [13].

Table I: Denoising results using *Zebra* image.

σ	Noisy	c-hyper	hyper	NSWT	curv	NSCT
10	28.11	**30.77**	30.45	26.32	26.39	29.58
15	24.58	**28.28**	27.83	24.09	24.63	27.17
20	22.09	**26.57**	26.16	22.86	23.42	25.65
25	20.15	**25.49**	25.15	22.04	22.89	24.56
30	18.56	**24.67**	24.38	21.41	22.26	23.69

Table II: Denoising results using *Baboon* image.

σ	Noisy	c-hyper	hyper	NSWT	curv	NSCT
10	28.14	29.44	**29.61**	26.32	26.14	29.02
15	24.61	27.27	**27.31**	24.25	24.31	26.62
20	22.12	25.74	**25.78**	23.24	23.72	25.12
25	20.18	24.30	**24.35**	22.58	23.61	24.08
30	18.59	**23.49**	23.47	22.06	23.43	23.32

Table III: Denoising results using *Leopards* image.

σ	Noisy	c-hyper	hyper	NSWT	curv	NSCT
10	28.14	**32.32**	32.26	28.88	29.80	31.05
15	24.61	30.15	**30.21**	27.33	28.43	28.89
20	22.12	28.62	**28.84**	26.25	27.50	27.48
25	20.18	27.51	**27.76**	25.28	26.66	26.41
30	18.59	26.55	**27.01**	24.40	25.99	25.52

5. DISCUSSION AND CONCLUSION

Hyperbolic shearlets illustrate the flexibility of the framework of wavelets with composite dilations to build redundant multiscale and multidirectional decomposition transforms endowed with special geometric features. They have particular utility when it comes to applications such as deconvolution [14], [15]. Yet the ability to deal with directional informations efficiently also proves to be highly effective at representing complex images as illustrated by their performance in denoising. In addition, the new filter design methodology that comes from the direct application of the A and B_ℓ structure matrices employed in this work is of interest by itself as it allows for very complicated spatial-frequency tiling to be constructed. Unlike competing methodologies, the degrees of flexibility of our approach allow for very redundant decompositions and excellent directional selectivity, which are the main reasons for the very good estimation performance we obtained. In addition, these multi-channel based implementations are highly efficient and parallelizable. In particular, given m filters, the algorithms takes only $O(mN^2 \log N)$ operations in a serial formulation for an $N \times N$ image and this is highly efficient compared to the nonsubsampled contourlet transform as timed in [8].

6. REFERENCES

[1] L. Jacquesa, L. Duvalb, C. Chauxc, G. Peyre, "A panorama on multiscale geometric representations, intertwining spatial, directional and frequency selectivity," *Signal Processing*, vol. 91, no. 12, pp. 2699-2730, Dec. 2011.

[2] S. Durand, "M-band filtering and non-redundant directional wavelets," *Applied Comput. Harmonic Anal.*, vol. 22, no. 1, pp. 124-139, 2007.

[3] K. Guo, W.-Q Lim, D. Labate, G. Weiss and E. Wilson, "Wavelets with composite dilations", *Electron. Res. Announc. Amer. Math. Soc.*, vol. 10, pp. 78–87, 2004.

[4] K. Guo, W-Q. Lim, D. Labate, G. Weiss and E. Wilson, "The theory of wavelets with composite dilations", in: Harmonic Analysis and Applications, C. Heil (ed.), pp. 231–249, Birkhäuser, Boston, MA, 2006.

[5] K. Guo and D. Labate, "Optimally sparse multidimensional representation using shearlets", *SIAM J. Math. Anal.*, Vol. 9, pp. 298–318, 2007.

[6] F. Colonna, G. Easley, K. Guo, and D. Labate, "Radon Transform Inversion using the Shearlet Representation", *Appl. Comput. Harmon. Anal.*, vol. 29, no. 2 pp. 232–250, 2010.

[7] G. R. Easley, D. Labate, F. Colonna, "Shearlet-Based Total Variation Diffusion for Denoising", *IEEE Trans. Image Proc.*, vol. 18, no. 2, pp. 260–268, 2009.

[8] G. Easley, W. Lim, and D. Labate, "Sparse Directional Image Representations using the Discrete Shearlet Transform", *Appl. Comput. Harmon. Anal.*, vol. 25, pp. 25–46, 2008.

[9] V. M. Patel, G. R. Easley, and D. M. Healy, Jr., "Shearlet-based deconvolution", *IEEE Trans. Image Proc.*, vol. 18, no. 12, pp. 2673–2685, 2009.

[10] S. Yi, D. Labate, G. R. Easley, and H. Krim, "A Shearlet approach to Edge Analysis and Detection", *IEEE Trans. Image Proc.*, vol. 18, no. 5, pp. 929–941, 2009.

[11] A. L. Cunha, J. Zhou, M. N. Do, "The nonsubsampled contourlet transform: Theory, design, and applications", *IEEE Trans. Image Processing*, vol. 15, no.10, pp. 3089–3101, 2006.

[12] G. Easley, D. Labate, "Critically sampled wavelets with composite dilations", *to appear in IEEE Trans. on Imag. Processing*, 2011.

[13] G. R. Easley, D. Labate, V. M. Patel, "Directional multiscale processing of images using wavelets with composite dilations", *preprint*, 2011.

[14] J. Chung, G. R. Easley, and D. P. O'Leary, "Windowed Spectral Regularization of Inverse Problems", *to appear in SIAM Journal on Scientific Computing*, 2011.

[15] K. Egan, Y-T Tseng, N. Holzschuch, F. Durand, R. Ramamorthi, "Frequency Analysis and Sheared Reconstruction for Rendering Motion Blur", *to appear in ACM SIGGRAPH*, 2011.

[16] P. Schiske, "Zur frage der bildrekonstruktion durch fokusreihen", *Proc. Eur. Reg. Conf. Electron. Microsc., 4th*, pp. 1–145, 1968.

[17] P. Schiske, "Image processing using additional statistical information about the object", *In P. W. Hawkes, ed., Image Processing and Computer Aided Design in Electron Optics*. Academic Press, New York, 1973.

[18] G. Harikumar, and Y. Bresler, "FIR perfect signal reconstruction from multiple convolutions: minimum deconvolver orders", *IEEE Transactions on Signal Proc.*, vol. 46, no. 1, pp. 215–218, 1998.

[19] G. R. Easley, and D. F. Walnut, "Local multichannel deconvolution", *J. Math. Imaging Vision*, vol. 18, pp. 69-80, 2003.

[20] F. Colonna, and G. R. Easley, "The multichannel deconvolution problem: a discrete analysis", *J. Fourier Anal. Appl.*, vol. 10, pp. 351–376, 2004.

[21] G. R. Easley, V. M. Patel, and D. M. Healy, Jr., "An M-channel directional filter bank compatible with the contourlet and shearlet frequency tiling," in Wavelets XII, San Diego, CA, 2007.

[22] S. Mallat, *A Wavelet Tour of Signal Processing*, Academic Press, San Diego, 1998.

[23] J. L. Starck, E.J. Candes, D.L. Donoho, "The curvelet Transform for Image Denoising", *IEEE Trans. on Image Processing*, vol. 11, no. 6, pp 670-684, 2002.